International Journal of Nanomedicine

Dovepress
open access to scientific and medical research

Open Access Full Text Article

ORIGINAL RESEARCH

# Investigation of the "Nose-to-Brain" Pathways in Intranasal HupA Nanoemulsions and Evaluation of Their in vivo Pharmacokinetics and Brain-Targeting Ability

Yueyao Jiang[1], Yichuan Jiang[1], Zhiying Ding[2], Qian Yu[1]

[1]Department of Pharmacy, China-Japan Union Hospital, Jilin University, Changchun, 130033, People's Republic of China; [2]Department of Pharmacology, School of Pharmaceutical Sciences, Jilin University, Changchun, 130021, People's Republic of China

Correspondence: Qian Yu, Department of Pharmacy, China-Japan Union Hospital, Jilin University, Changchun, 130033, People's Republic of China, Tel +86 13664419002, Email yuqian@jlu.edu.cn



**Purpose:** While developing huperzine A (HupA) to explore new approaches to treating Alzheimer's disease (AD), intranasal administration was proposed as an alternative route to deliver drugs into the brain. This study aimed to prepare nanoemulsions (NEs) of HupA to investigate their potential "nose-to-brain" pathways and to evaluate their pharmacokinetic and brain-targeting parameters.

**Methods:** HupA-NE and Lf-HupA-NE that underwent surface modification with lactoferrin (Lf) were characterized to determine various physicochemical properties, such as their size, PDI, zeta potential, pH, and loading efficiency; in addition, transmission electron microscopy and stability assessments were performed. We utilized an aggregation-caused quenching (ACQ) probe to monitor intact NEs in the brains of olfactory nerve transection model and normal rats. Immunohistochemistry, pharmacokinetic and targeting index analyses were performed to investigate the in vivo effects of HupA-NE and Lf-HupA-NE.

**Results:** Based on the live imaging results, HupA-NE and Lf-HupA-NE could be transported into the brain via nerve and blood circulation pathways. Immunohistochemical staining tests demonstrated that the efflux proteins P-gp, MRP1, and BCRP were expressed in brain tissue. NEs can inhibit efflux pumps to improve drug concentrations in the brain. The findings of this study showed that NEs (especially Lf-HupA-NE) had better pharmacokinetic profiles and a better nose-to-brain drug transport efficiency than free HupA.

**Conclusion:** The newly designed formulations might contribute to the transport and accumulation of HupA to achieve therapeutic results. The delivery system may be a promising strategy for the brain-targeted delivery of HupA.

**Keywords:** intranasal administration, nanoemulsions, "nose-to-brain" pathway, pharmacokinetics

## Introduction

Alzheimer's disease (AD) is an acquired disorder that involves cognitive and behavioral disabilities within elderly populations.[1–3] Treatment with huperzine A (HupA), found in the Chinese herb *Huperzia serrata*,[4] results in significant improvements in memory and cognitive functions. It has been reported that HupA can effectively decrease oxidative injury by upregulating the activities of antioxidant enzymes, suppressing the accumulation of β-amyloid peptides, ameliorating mitochondrial dysfunction, and enhancing the viability of neurons.[5] In the available treatments of AD, HupA is administered orally and through injections. However, the existing forms of HupA (such as tablets, capsules, and injectables) result in peripheral nervous system and gastrointestinal side effects.[6,7] The drug's therapeutic effect is reduced by a lack of brain selectivity and a lower concentration of drug in the brain due to the blood–brain barrier (BBB).[3] P-glycoprotein (P-gp), breast cancer resistance protein (BCRP) and multidrug resistance-associated protein 1 (MRP1)[8] are members of the adenosine triphosphate-binding cassette (ABC) transporter superfamily of critical efflux transporters in brain tissue. Efflux transporters can pump most exogenous substances from the CNS. These efflux transporters can rapidly remove these compounds back to the systemic circulation or even block their complete transcytosis.[9] Hence, a suitable delivery method for HupA treatments is greatly needed. The intranasal (IN) route has emerged as an alternative

Received: 12 April 2022
Accepted: 15 July 2022
Published: 4 August 2022

**Graphical Abstract**

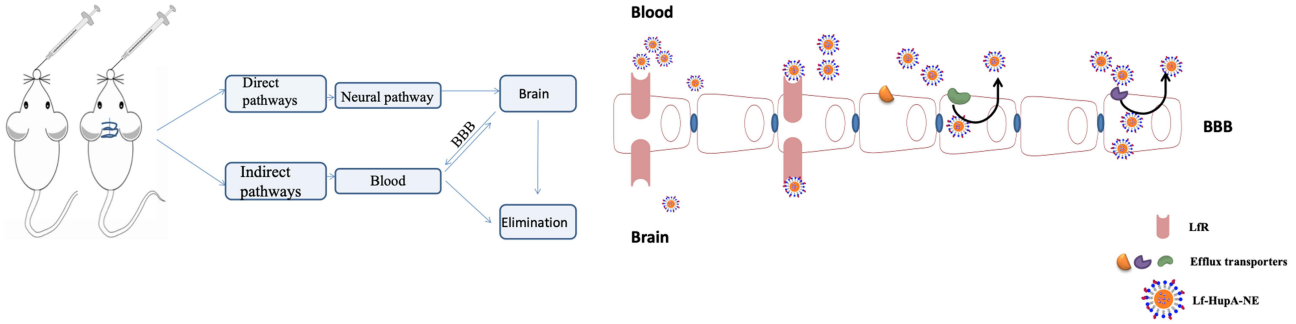


approach over oral and injected administration. When given via the IN route, drugs can partly bypass the BBB, traveling directly from the nasal cavity to the brain via the olfactory and trigeminal nerves.[10–12] Moreover, the IN route provides a convenient and noninvasive means of drug administration, facilitating good compliance.[13] Nevertheless, the development of IN routes is limited by many factors regarding macromolecular drugs, such as their nasal mucociliary clearance, enzymatic degradation, nasal toxicity and difficulty in passing the nasal mucosa.[14,15] Considering the above limitations, nanoemulsions (NEs) have been utilized to increase effective drug transport by prolonging retention, improving the permeation of mucosal epithelia, and protecting payloads from biological/chemical degradation.[16,17] However, the fate of integral transportation of NEs from the nose to the brain and the possible pathways remain unclear. This difficulty is due to the lack of functional tools that can trace the transportation of intact NEs. Recently, the School of Pharmacy, Fudan University, demonstrated sensitive aggregation-caused quenching (ACQ) probes to discriminate nanoparticle-associated signals from those of free probes in vivo. The ACQ probes emit fluorescent signals in lipid matrix NEs and are instantly and completely quenched upon contact with water.[18,19] Our group developed and characterized a HupA-NE and a targeted HupA-NE that was modified with lactoferrin (Lf) for intranasal administration. Lf is a mammalian cationic iron-binding glycoprotein that binds to Lf receptors; these receptors are highly expressed in brain endothelial cells and neurons.[20,21]

In this study, ACQ probes were utilized to monitor the possible pathways of nasal NEs in vivo. In addition, we investigated the influence of NEs on multidrug efflux transporters in the brain. Drug-time concentrations and pharmacokinetic parameters of vital organs were helpful for evaluating the beneficial effects of intranasal NEs.

# Materials and Methods

## Materials

HupA was supplied by MULTI SCIENCES (Hangzhou, China). Propylene glycol monocaprylate (Capryol 90) and caprylocaproyl macrogolglycerides (Labrasol) were purchased from Gattefossé (Saint-Priest, France). Propan-2-yl tetradecanoate (IPM) was provided by Sinopharm Chemical Reagent Co., Ltd. (Shanghai, China). Anti-P-gp antibody [EPR10364] (ab168337), anti-BCRP/ABCG2 antibody [EPR20080] (ab207732), anti-MRP1 antibody [EPR21062] (ab233383), and goat anti-rabbit IgG (H+L)-horseradish peroxidase-conjugated (ab181448) secondary antibody were purchased from Abcam (Cambridge, UK). The water-quenching near infrared fluorescent probe P2 (λabs/λem = 720 nm/740 nm) was provided by the School of Pharmacy, Fudan University.

## Animals

In vivo studies were carried out on adult Wistar rats that weighed 200±20 g and were purchased from the Experimental Animal Center of Jilin University (Changchun, China). All animal procedures were conducted in strict accordance with the National Institutes of Health Guide for the Care and Use of Laboratory Animals and were approved by the Animal

Care and Use Committee of the College of Pharmacy of Jilin University (permit number: 20190056; application date: Sept. 2019; ending date: Sept. 2020; Changchun, China).

## HPLC Analysis

A C18 column (COSMOSIL packed column 5C18-MS-11, SHIMADZU, Japan) was utilized for drug separation, and methanol combined with water (43:57) was used as the mobile phase. One milliliter of triethanolamine was added to 1000 mL of water until a pH of 7 was reached. The flow rate was 1 mL/min, and the retention time was 15.6 min. The samples were detected at 308 nm, and the assays were performed at ambient temperature. The basic parameters of HPLC method validation in vitro and in vivo were illustrated in the Supplementary Material.

## Preparation of HupA-NE and Lf-HupA-NE

Based on the prior data obtained from the phase diagrams that were generated and the Box–Behnken design (BBD), our group prepared an optimal HupA-NE and Lf-HupA-NE. HupA was dissolved in a mixture of oil phase 3.00% IPM and 3.81% Capryol 90. A total of 26.67% surfactant (Cremophor EL) and 13.33% cosurfactant (Labrasol) were added to the oil mixture. Double-distilled water (53.19%) was added to the mixture dropwise with constant stirring using a magnetic stirrer at ambient temperature. The final HupA concentration for HupA-NE was 5 mg/mL. The positively charged Lf was dissolved in the water phase to adsorb the HupA-NE surface. The optimum concentration of Lf was 5 mg/mL. The highly lipophilic probe ACQ-P2 (λabs/λem=720/740 nm), which was dissolved in the oil phase and encapsulated within HupA-NE and Lf-HupA-NE, was used as a tool for tracking the presence of nanoparticles in vivo. In a previous study, the formulations were characterized and evaluated for their particle size distribution, zeta potential, in vitro release and stability and were examined through transmission electron microscopy.[21]

## Characterization of HupA-NE and Lf-HupA-NE

### Droplet Size, Polydispersity Index (PDI) and Zeta Potential Analysis

NE formulations (0.1 mL) were dispersed in 50 mL distilled water. The globule size and PDI were measured by dynamic light scattering (Nano-ZS90, Malvern, UK). The zeta potentials were also measured by photon correlation spectroscopy using a Zetasizer (Nano-ZS90, Malvern, UK). All measurements were carried out at 25°C.[22]

### Transmission Electron Microscopy Analysis and pH Measurement

A drop of each diluted HupA-NE and Lf-HupA-NE was placed onto a 300-mesh copper grid and stained with 2% (w/v) phosphotungstic acid (PTA) for 5 min at room temperature. Excess staining reagent was removed with filter paper. The samples were situated on the sample holder and analyzed with a transmission electron microscope (TEM, Hitachi, Tokyo, Japan). The absorption and interaction of drugs with the nasal mucosa is influenced by the pH of the formulations for nasal delivery. A pH meter was used to test the pH of the NEs.

### Determination of HupA Loading Efficiency in HupA-NE and Lf-HupA-NE

Then, 0.5 mL of HupA-NE or Lf-HupA-NE in a 50-mL volumetric flask was diluted in methanol to volume. The resulting solution (1 mL) was filtered through a 0.45 μm membrane filter and subjected to HPLC analysis.

### Stability Assessment

The stability of the NEs was assessed by the size distribution, loading efficiency and physical appearance of the NEs at 4°C and room temperature for 0.5, 1, and 3 months.

## Nose-to-Brain Delivery

An olfactory nerve transection model was established in rats to study the "nose-to-brain" pathways traveled by NE formulations. Rats underwent fasting overnight and were anesthetized by an intraperitoneal injection of 10% chloral hydrate. The rat heads were fixed with a brain stereotaxic apparatus and disinfected with iodine. An incision was made along the midline of the two ears, and the exposed skull was wiped with sterile skimmed cotton. The incision was positioned at the intersection of the anteroposterior at 7–8 mm and the mediolateral at 2 mm (AP: +8 mm, ML: ±2 mm).

The dura covering the surface of both olfactory bulbs was pierced. A flexible Teflon blade was inserted, and all olfactory axons were cut. After the surgery was complete, the incision was sutured. Then, the animals were placed back in their cages after fully recovering from the anesthesia. The olfactory nerve transection model and normal rats were nasally administered 50 μL of P2 aqueous solution, P2-HupA-NE or P2-Lf-HupA-NE. Beginning 1 h after administration, IVIS Spectrum Live Imaging was utilized at maximum excitation/emission wavelengths (P2: 720/740 nm) to obtain live in vivo images of the dorsal side of the animals.

## Immunohistochemistry (IHC)

Twenty male Wistar rats were randomly divided into the following groups: (1) rats in the control group were intranasally administered 50 μL of 0.9% NaCl solution; (2) rats in the HupA group were intranasally administered 50 μL of HupA solution at a dose of 1.25 mg/kg; (3) rats in the HupA-NE group were intranasally administered 50 μL of HupA at a dose of 1.25 mg/kg; and (4) rats in the Lf-HupA-NE group were intranasally administered 50 μL of HupA at a dose of 1.25 mg/kg. The rats received intranasal doses continuously for 14 days. After 14 days, the animals were anesthetized, and their hearts were perfused with saline. The brains were removed and fixed in 4% formaldehyde for hematoxylin and eosin (HE) staining and immunohistochemical analysis. The rat brains were fixed in 4% formaldehyde for 3 days and embedded in paraffin. Brain sections (5 μm thick) were stained with HE, deparaffinized, rehydrated and immunohistochemically stained using the DAB method. The slides were incubated overnight at 4°C with primary antibodies against P-gp, BCRP, and MRP1 and then labeled with streptavidin peroxidase. The immunoreactive proteins were visualized using an optical microscope (OLYMPUS, Japan) at 100× magnification. All staining was assessed by pathologists who were blinded to the sample origins. The widely accepted German semiquantitative scoring system that considers the staining intensity and area extent was used. Each specimen was assigned a score according to the intensity (no staining =0, weak staining =1, moderate staining =2, strong staining =3) and proportion of stained cells (0% =0, 1–24% =1, 25–49% =2, 50–74% =3, 75–100% =4). The final immunoreactive score was determined by multiplying the intensity score by its extent, and the scores ranged from 0 (minimum score) to 12 (maximum score).

## Pharmacokinetics and Targeting Index Analysis

Male Wistar rats (n=55) were randomly divided into the following groups: nasal administration of HupA-NE or Lf-HupA-NE and gavage of HupA aqueous solution. The rats in one formulation were further divided into 11 time points with five rats in each point. The rats were anesthetized by intraperitoneal injection of 10% chloral hydrate. Fifty microliters of HupA-NE or Lf-HupA-NE was slowly and gently administered via a PE 10 tube attached to a syringe, which was inserted 1 cm into the nostril.[23] The blood and vital organs (lung, liver, kidneys, heart, spleen, and brain) were excised, isolated and weighed at 5 min, 15 min, 30 min, 1 h, 2 h, 4 h, 6 h, 8 h, 12 h, 16 h and 24 h. The tissues were homogenized in 1% perchloric acid using a tissue homogenizer. The plasma was added to 6% perchloric acid. The supernatant was separated, and the proteins were removed by centrifugation and filtration. Two milliliters of ethyl acetate was added to the supernatant, and the pH was adjusted to 11.8 by 2 mol/L NaOH solution. The HupA in the supernatant was extracted using ethyl acetate. The ethyl acetate extracts were dried using nitrogen, redissolved in methanol, and injected into the HPLC.

Pharmacokinetic analysis of intranasal administration of NEs and oral HupA solution was performed and compared using the computer program DAS 2.0. The relative uptake rate (Re) and peak concentration ratio (Ce) of distribution parameters were calculated by pharmacokinetic parameters that were used for the evaluation of target ability. The drug targeting index (DTI) was used to evaluate the brain targeting of the Lf-modified NE.

$$Re_{NEs} = \frac{\left(AUC_{(0-t)}\right)_{NEs}}{\left(AUC_{(o-t)}\right)_{HupA\ solution}}$$

$$Ce_{NEs} = \frac{\left(C_{max}\right)_{NEs}}{\left(C_{max}\right)_{HupA\ solution}}$$

$$DTI = \frac{\left(AUC_{brain}/AUC_{plasma}\right)_{Lf-HupA-NE}}{\left(AUC_{brain}/AUC_{plasma}\right)_{HupA-NE}}$$

# Results

## Characterization of HupA-NE and Lf-HupA-NE

The physicochemical properties of the NEs are shown in Figure 1. The droplet sizes of HupA-NE and Lf-HupA-NE were 14.39±0.29 nm (PDI = 0.086±0.002) and 16.74±0.47 nm (PDI = 0.066±0.001), respectively. The zeta potentials of HupA-NE and Lf-HupA-NE were −14.69±0.35 and +5.67±0.39 mV, respectively. TEM (Figure 2) revealed that the nanodroplets were spherical with a uniform distribution, and the droplet sizes were consistent with the results obtained by photon correlation spectroscopy. The pH values measured by a pH meter were 5.75 and 6.15, respectively, which were within the normal nasal pH range, reducing damage to the nasal mucosa. The HupA loading efficiency was found to be 4.94±0.127 mg/mL and 4.87±0.239 mg/mL in HupA-NE and Lf-HupA-NE, respectively. The stability assessments of the appearance, particle size and loading efficiency for 0.5, 1 and 3 months at 4°C and room temperature are shown in Table 1. There was no significant statistical variation in the particle size or drug loading efficiency. There was a minimal increase in the particle size and an acceptable decrease in the drug loading efficiency. Visual observations of HupA-NE and Lf-HupA-NE revealed that they were still clear and transparent.

## Nose-to-Brain Delivery

Figure 3 shows the retention of P2 aqueous solution, P2-HupA-NE and P2-Lf-HupA-NE in the brains of olfactory nerve transection model rats and normal rats. The live images that were obtained after the P2 quenched solution was administered showed no fluorescence. Since no fluorescent signal was observed, the interference from the quenched probes was eliminated. Following the destruction of the olfactory bulb in model rats, the distribution of fluorescence was still detectable in brain areas after intranasal administration. It was suggested that some HupA-NE and Lf-HupA-NE could be absorbed into the blood circulation and could be transported into the brain by the indirect nose-to-brain pathway. The intense P2 signal in the normal group of rats had a higher retention than that in the model group. It was implied that HupA-NE and Lf-HupA-NE were transported into the brain both directly (via the olfactory nerve) and indirectly (through

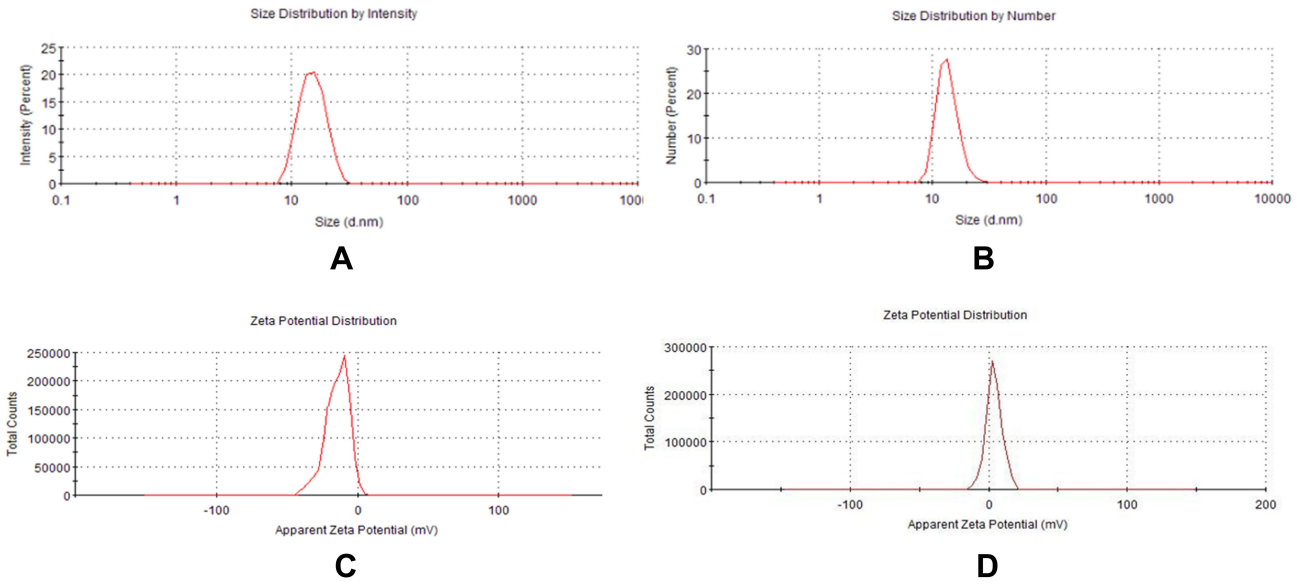


**Figure 1** Characterization parameters of optimized NEs. (**A** and **B**) Droplet size distribution of HupA-NE and Lf-HupA-NE. (**C** and **D**) Zeta potential of HupA-NE and Lf-HupA-NE.

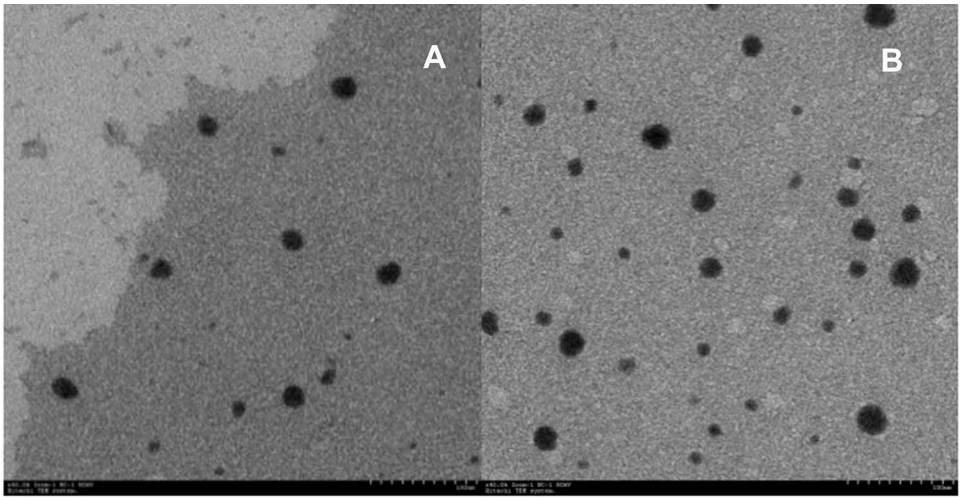


**Figure 2** TEM of (**A**) HupA-NE and (**B**) Lf-HupA-NE.

the bloodstream). The intensity and ranges of P2 signals were found in the following order: Lf-HupA-NE > HupA-NE, and this was due to a high percentage of translocation through the nose to the brain.

## In vivo Efflux Study

Immunohistochemistry studies were performed to investigate the effects of HupA-NE and Lf-HupA-NE on the expression of efflux proteins in brain tissue, as shown in Figure 4A. The positive products were expressed as a brown specific cellular stain mainly on the cell membrane and cytoplasm. Tissue sections were analyzed by the degree of staining using the scoring method. The scoring system used in immunohistochemical analysis was feasible.[24] Figure 4B shows that HupA solution altered the expression of p-gp, MRP1 and BCRP efflux transporters, which have an important role in cellular protection because of their ability to remove xenobiotics and endogenous substrates accumulated in cells. The protein expression levels of p-gp, MRP1 and BCRP were higher in the HupA aqueous solution group than in the blank control group. The compound of HupA might be the substrates of these efflux transporters. All scores in the NE groups

**Table 1** Stability of HupA-NE and Lf-HupA-NE (n =3)

| Nanoemulsion | Temperature (°C) | Time (Month) | Appearance | Size (nm) | Drug Loading Efficiency (mg/mL) |
|---|---|---|---|---|---|
| HupA-NE | 4 | 0.5 | Clear and transparent | 15.92±0.14 | 4.94±0.10 |
| | | 1 | Clear and transparent | 16.64±0.31 | 4.93±0.13 |
| | | 3 | Clear and transparent | 18.67±0.26 | 4.91±0.31 |
| | 25 | 0.5 | Clear and transparent | 17.31±0.18 | 4.98±0.15 |
| | | 1 | Clear and transparent | 20.97±0.21 | 4.91±0.37 |
| | | 3 | Clear and transparent | 22.27±0.37 | 4.83±0.39 |
| Lf-HupA-NE | 4 | 0.5 | Clear and transparent | 16.95±0.16 | 4.96±0.13 |
| | | 1 | Clear and transparent | 17.12±0.11 | 4.89±0.38 |
| | | 3 | Clear and transparent | 17.45±0.19 | 4.86±0.73 |
| | 25 | 0.5 | Clear and transparent | 19.31±0.33 | 4.88±0.18 |
| | | 1 | Clear and transparent | 22.55±0.51 | 4.85±0.61 |
| | | 3 | Clear and transparent | 23.87±0.75 | 4.71±0.56 |

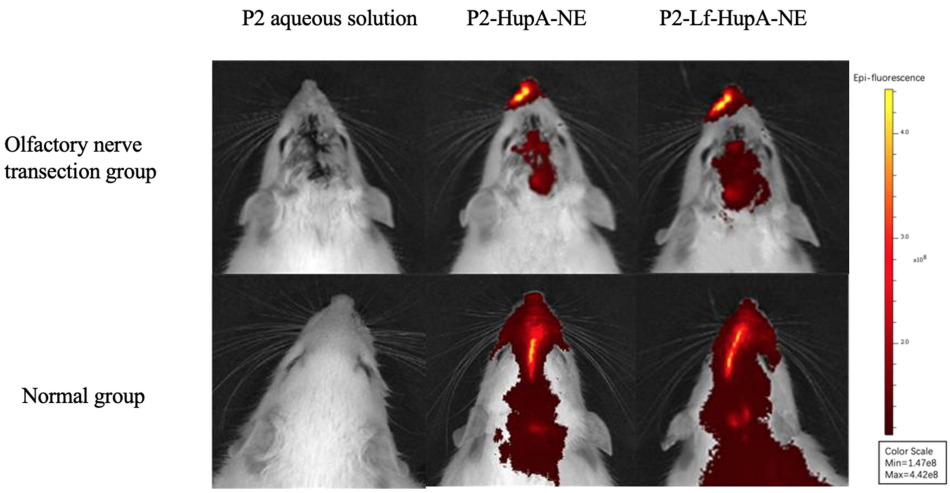


**Figure 3** Live imaging in the brains of P2 aqueous solution, P2-HupA-NE and P2-Lf-HupA-NE after intranasal administration to olfactory nerve transection model rats and normal rats.

were lower than those in the HupA aqueous solution group. The HupA-NE group scored lower than the blank control group; presumably, the preparation might inhibit the expression of the efflux proteins. The Lf-HupA-NE group scored lower than the HupA aqueous solution group but higher than the HupA-NE group. Lf-HupA-NE inhibited the efflux transporter protein levels, but the intensity of the inhibitory effect was weaker than that of HupA-NE.

## Measurement of Time–Concentration Relationships

The time–concentration curves of blood and vital organs are shown in Figure 5. The time–concentration curve profiles showed that the peak time of nasal HupA-NE and Lf-HupA-NE was faster than that of the gavage HupA aqueous solution in blood and vital organs. The concentration (C) of the drug in brain tissue at the same time point was in the following order: CLf-HupA-NE>CHupA-NE>CHupA aqueous solution. The duration of action in the brain (T) was in the following order: TLf-HupA-NE>THupA-NE>THupA aqueous solution. The peak concentrations were higher in the heart, liver, spleen and kidney for the HupA solution by gavage, while the peak concentrations were higher in the brain and lung for the NE formulations, suggesting that the NEs changed the distribution of the drug in vivo.

## Pharmacokinetic Parameters and Targeting Index Analysis

The pharmacokinetics of NEs were determined in Wistar rats through the intranasal route in comparison to intragastric pure drug. The pharmacokinetic parameters are shown in Table 2. There was a significant increase in brain Cmax and area under the curve (AUC(0-t)) for all intranasal NE formulations. The time to reach the maximum concentration (Tmax) in the brains of the HupA-NE and Lf-HupA-NE groups was faster than that in the HupA solution group. The MRT(0-t) and t1/2 of the NEs were significantly prolonged, and the clearance rate (CL/F) was reduced, indicating that the HupA nano-formulations entered the brain and significantly prolonged the duration of action in the brain with sustained release. The alteration of various brain pharmacokinetic parameters by Lf confirmed that Lf-HupA-NE outperformed HupA-NE. The Lf-HupA-NE formulation changed the distribution of HupA-NE in vivo. The AUC(0-t) of Lf-HupA-NE was smaller than that of HupA-NE in all tissues except the brain. The heart, liver and kidney peak concentrations of NEs were significantly lower than those of the HupA aqueous solution, and the rate of clearance was higher in the liver and kidneys. NEs not only improve brain targeting but also reduce the cardiac, hepatic and renal toxicity of the drug. The development of HupA into NEs, especially brain-targeted Lf-HupA-NE, can result in a specific distribution of the drug in vivo.

The larger quantitative value of Ce has a more desirable change in the drug distribution. Re represents the selectivity of the pharmaceutical preparation in tissues. The targeting indices Ce and Re were both greater than 1 in the brain,

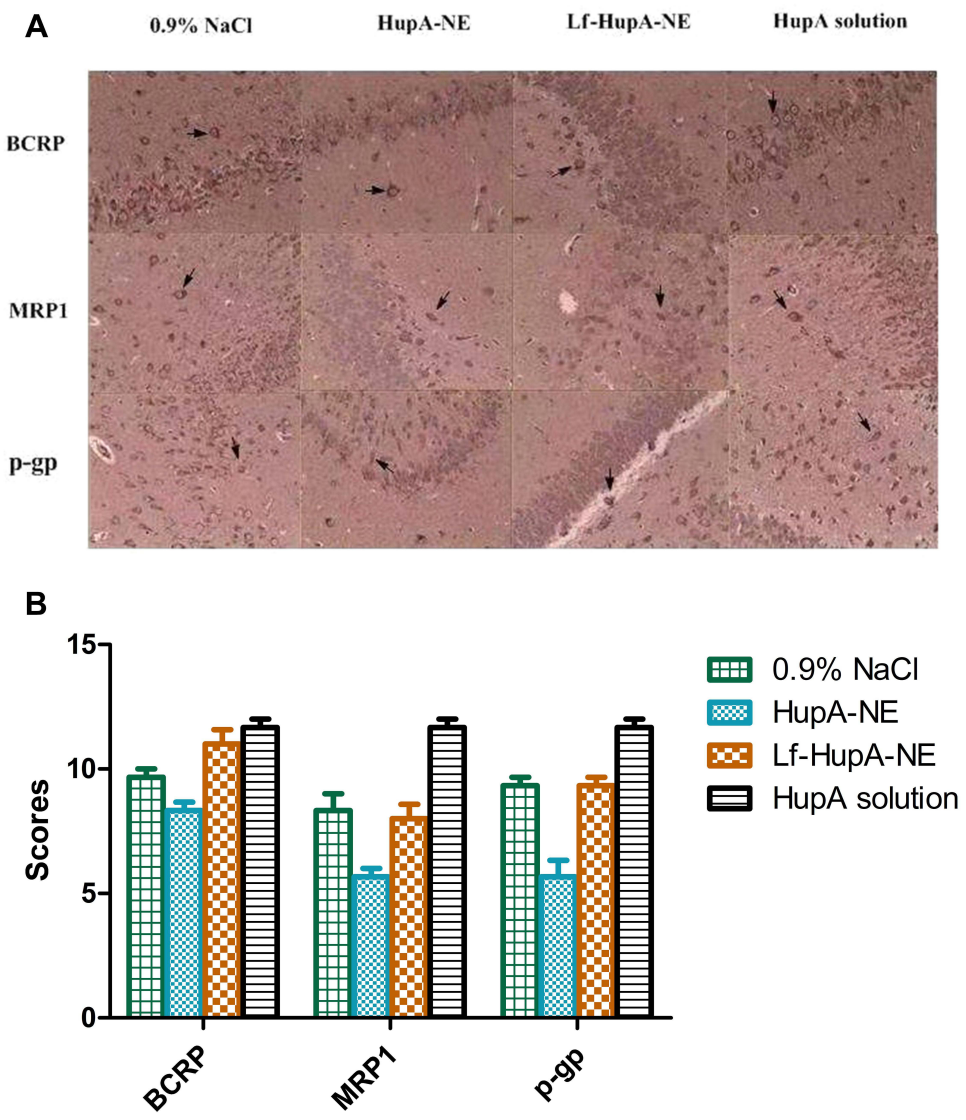


**Figure 4** Effects of HupA-NE and Lf-HupA-NE on the expression of efflux proteins in brain tissue (**A**) Immunohistochemical protein staining at 100× magnification; (**B**) immunoreactive score. Values represent the mean±SD (n=5).

indicating that the nasally administered NE groups had an ability to target the brain compared to that of the gavage aqueous group. The results of Ce and Re were shown below. The DTI of Lf-HupA-NE was 2.61, so the Lf-HupA-NE has stronger brain targeting than HupA-NE.

$$Ce_{HupA-NE} = \frac{(C_{max})_{HupA-NE}}{(C_{max})_{HupA\ solution}} = 3.38$$

$$Ce_{Lf-HupA-NE} = \frac{(C_{max})_{Lf-HupA-NE}}{(C_{max})_{HupA\ solution}} = 3.83$$

$$Re_{HupA-NE} = \frac{(AUC_{(0-t)})_{HupA-NE}}{(AUC_{(o-t)})_{HupA\ solution}} = 4.32$$

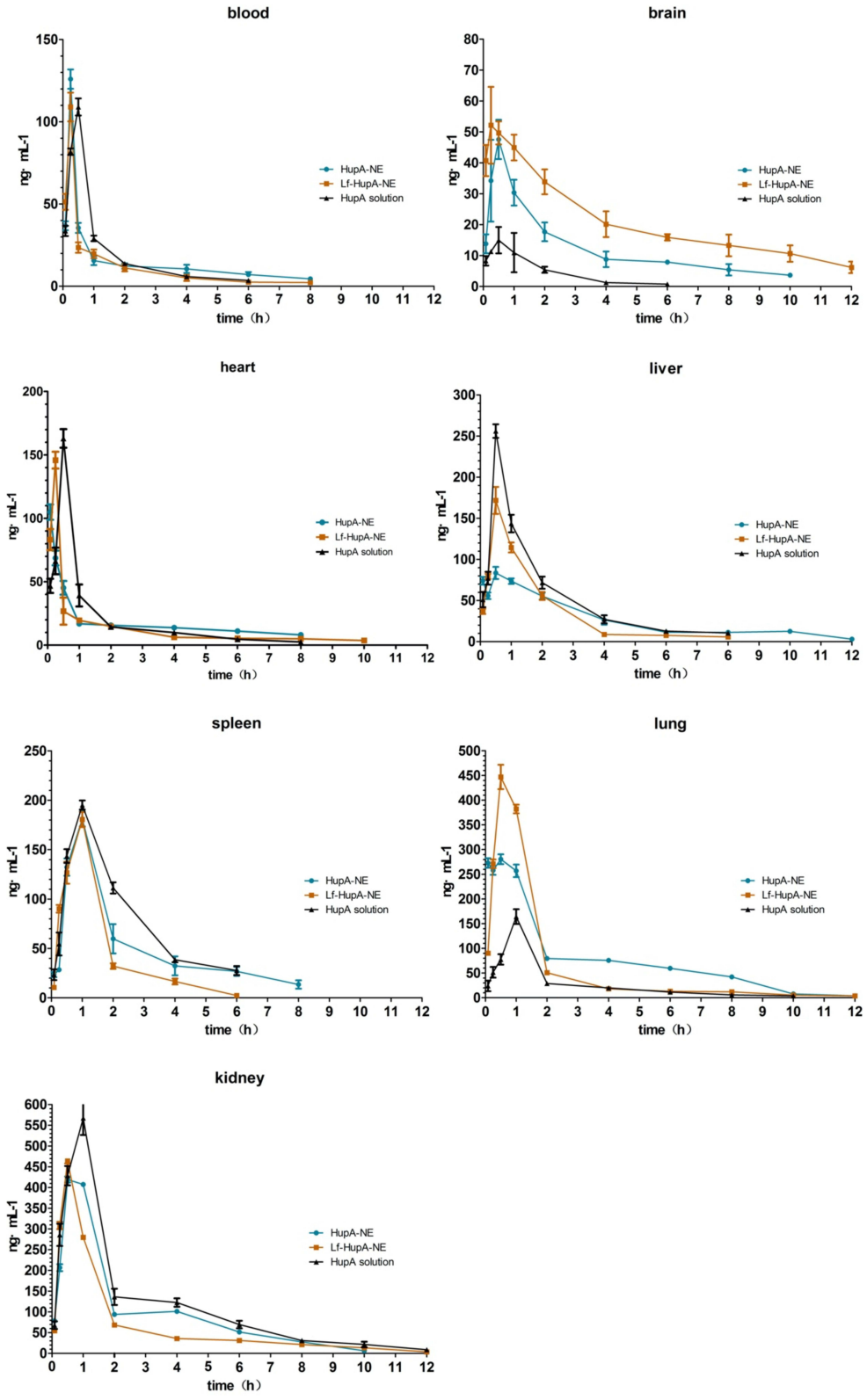


**Figure 5** The time–concentration curves of blood and vital organs. Values represent the mean±SD (n=5).

**Table 2** Pharmacokinetic Parameters of HupA-NE and Lf-HupA-NE (n =5) *$p$<0.05

| | Cmax (ng/mL) | | | AUC(0-t) (ng/mL*h) | | | Tmax (h) | | |
|---|---|---|---|---|---|---|---|---|---|
| | **Nasal HupA-NE** | **Nasal Lf-HupA-NE** | **Gavage HupA Solution** | **Nasal HupA-NE** | **Nasal Lf-HupA-NE** | **Gavage HupA Solution** | **Nasal HupA-NE** | **Nasal Lf-HupA-NE** | **Gavage HupA Solution** |
| Brain | 50.54±0.81* | 57.29±3.61* | 14.97±4.25 | 123.63±12.96* | 245.09±17.45* | 28.60±5.72 | 0.41±0.14 | 0.33±0.14 | 0.5±0.00* |
| Plasma | 125.93±10.21 | 108.99±15.09 | 109.01±8.99 | 114.04±5.69 | 86.86±5.24 | 119.05±10.06* | 0.25±0.00 | 0.25±0.00 | 0.5±0.00* |
| Heart | 104.92±0.07 | 145.85±6.63* | 162.95±7.33* | 138.46±0.89 | 124.82±1.29 | 163.28±5.85* | 0.083±0.00 | 0.25±0.00 | 0.5±0.00* |
| Liver | 84.73±5.29 | 171.72±16.48* | 256.09±8.27* | 316.29±13.34 | 292.27±14.82 | 423.62±22.93* | 0.36±0.24 | 0.5±0.00 | 0.5±0.00 |
| Spleen | 181.10±7.58 | 180.48±7.64 | 195.15±4.58 | 415.82±12.03* | 286.32±16.03 | 485.35±5.11* | 1.00±0.00 | 1.00±0.00 | 1.00±0.00 |
| Lung | 280.41±9.96 | 446.86±24.62* | 173.18±14.13 | 879.23±34.37* | 661.38±46.78* | 287.58±13.04 | 0.50±0.00 | 0.50±0.00 | 1.00±0.00* |
| Kidney | 419.33±7.14 | 463.87±5.93 | 567.41±40.60* | 1021.21±10.23 | 762.39±7.73 | 1354.02±33.28* | 0.50±0.00 | 0.50±0.00 | 1.00±0.00* |
| | **CL/F (mL*h)** | | | **MRT(0-t) (h)** | | | **t1/2 (h)** | | |
| | **Nasal HupA-NE** | **Nasal Lf-HupA-NE** | **Gavage HupA Solution** | **Nasal HupA-NE** | **Nasal Lf-HupA-NE** | **Gavage HupA Solution** | **Nasal HupA-NE** | **Nasal Lf-HupA-NE** | **Gavage HupA Solution** |
| Brain | 8.61±0.81 | 4.35±0.38 | 42.63±7.93* | 3.03±0.19* | 4.07±0.14* | 1.49±0.12 | 3.94±0.47* | 4.47±1.97* | 1.27±0.16 |
| Plasma | 8.40±1.68 | 12.34±0.99 | 9.88±0.89 | 2.35±0.13 | 1.71±0.32 | 1.31±0.12 | 5.01±2.61* | 3.31±2.03 | 1.77±0.83 |
| Heart | 6.09±0.26 | 7.52±1.33 | 7.26±0.05 | 2.75±0.07 | 2.44±0.14 | 1.60±0.05 | 5.69±0.72 | 8.02±5.01* | 2.21±0.68 |
| Liver | 3.81±0.15 | 4.21±0.22 | 2.88±0.15* | 3.33±0.04* | 1.69±0.03 | 1.95±0.04 | 0.36±0.24 | 0.5±0.00 | 0.5±0.00 |
| Spleen | 2.68±0.18 | 4.32±0.25* | 2.45±0.03 | 2.47±0.05 | 1.42±0.03 | 2.03±0.06 | 1.00±0.00 | 1.00±0.00 | 1.00±0.00 |
| Lung | 1.41±0.06 | 1.83±0.13 | 4.03±0.09* | 3.06±0.05* | 1.79±0.15 | 2.28±0.06 | 1.71±0.25 | 3.66±0.25* | 2.49±0.13 |
| Kidney | 1.17±0.00 | 1.54±0.04* | 0.91±0.02 | 2.55±0.04 | 2.39±0.04 | 2.78±0.05 | 2.13±0.14 | 3.42±0.82 | 2.10±0.10 |

$$Re_{Lf-HupA-NE} = \frac{\left(AUC_{(0-t)}\right)_{Lf-HupA-NE}}{\left(AUC_{(o-t)}\right)_{HupA\ solution}} = 8.57$$

## Discussion

The droplet size, PDI and zeta potential are important physicochemical properties of NEs.[25] The transport of HupA from the nasal formulations to the brain is associated with a small globule size. Formulations showed nanoscale droplet sizes less than 20 nm with a low polydispersity index. Nanosized droplets have a greater surface area and high free energy, assuring that higher and faster drug permeation and absorption occurs.[26] Lf is an iron-binding glycoprotein that belongs to the transferrin family and carries a positive charge.[27] There are negative charges in the BBB that can adsorb positive charges. Lactoferrin receptor (LfR) is highly expressed in brain neurons and endothelial cells that are connected with AD.[28–30] Negatively charged HupA-NE was modified with the ligand Lf to enhance the nose-to-brain delivery of Lf-HupA-NE after intranasal administration.[31–33] Although Lf-HupA-NE has a lower value of zeta potential than that of other NEs, Kakumanu et al stated that a lower zeta potential maintained the stability and efficacy of nanodroplets.[34] The pH values of HupA-NE and Lf-HupA-NE were acceptable, within the limits of the human nasal pH range (4.5–6.5) and did not result in nasal irritation upon intranasal administration.[35] The stability of the NEs was evaluated based on whether the NEs maintained their size distribution and based on the loading efficiency and physical appearance of NEs, and the test evaluations were performed at 4°C and room temperature for 0.5, 1, and 3 months. The stability of NEs for the longer period was due to the cosurfactant effect, which imparted stability to the formulation as the result of their lower globule sizes.

The interior section of the nasal cavity has a neuronal network and blood vessels. Our group tried to determine the pathways by which NEs enter the brain through nasal administration. Tracking the transportation of NEs provided information that was very important for elucidating the mechanisms of the nose-to-brain delivery of HupA-NE and Lf-HupA-NE. The in vivo fate of NEs can be accurately monitored by using a novel environment-responsive fluorescent probe. Based on the maximum excitation/emission wavelengths, P2 was employed in this study for live imaging. Some signals were still observed in the olfactory nerve transection model rats, which might be due to NEs uptake into the brain also occurring through blood circulation. The rate and extent of P2 signals in the brains of the rats without operations were much higher, which suggested that nerves play an important role in the nose-to-brain pathways. This finding was consistent with the literature that reported that the main neuronal route of drug delivery is via olfactory and trigeminal sensory neurons.[36–38] The prepared NEs were in accordance with a previous report that nanoparticles with a particle size <20 nm can achieve extracellular transport from the nasal cavity to the brain.[39] Ejaj Ahmad reported that only NEs with a very small particle size can be translocated to the brain in an intact form and exhibit a prolonged duration of residence. The overall trend in the amount of NE retained was found to depend on particle size.[19] Therefore, HupA-NE and Lf-HupA-NE generally enter the brain from the nasal cavity by direct and indirect pathways. Drug transport via the BBB to the brain also occurs through blood circulation.

Previous studies have shown that efflux transporters weaken the brain uptake of drugs after nasal administration.[40–43] Thus, the effectiveness of therapeutic drugs may be restricted by ABC transporters, such as P-gp, BCRP and MRP1.[9] Efflux transporters pump most exogenous substances from the central nervous system (CNS). In vitro experiments that were performed in our laboratory verified that Pgp, BCRP, and MRP1 efflux transporters exist in brain vascular endothelial cells, and they are present to promote resistance to HupA when treating neurological diseases. The immunohistochemistry results revealed efflux transporter staining in brain tissues and found that P-gp, MRP1, and BCRP had strong reactions. HupA aqueous solution may increase the expression levels of P-gp, MRP1, and BCRP efflux transporters in the brain. Simultaneously, we found that the expression of efflux transporters treated with HupA-NE was lower than that treated with HupA solution. HupA-NE may be used to overcome drug resistance to improve AD therapy. It has been reported that NE can protect drugs by encapsulating and preventing the recognition of efflux transporters.[44,45] The pharmaceutical excipients of NEs can inhibit efflux pumps and increase drug absorption.[46,47] However, Lf-HupA-NE attenuated this inhibitory effect. There is no direct evidence to clarify whether Lf can inhibit the expression of exocytosis proteins. Lf plays critical roles in various physiological processes. It reduced ROS levels and upregulated the expression

of nuclear factor erythroid 2-related factor 2 (Nrf2) protein.[48] Some bioactive compounds increase the expression of efflux transporters through activation of the Nrf2-mediated signaling pathway.[49,50] Therefore, we speculated that Lf might reduce ROS production to induce the expression of efflux transporters, which are involved in the upregulated expression of Nrf2 proteins.

The time–concentration curve profiles indicated that the absorption rate of NEs nasal administration is faster than that of conventional gavage administration. Nasal administration of Lf-HupA-NE was superior to HupA-NE and gavage of HupA aqueous solution in terms of both drug distribution and sustained release in the brain. The highest concentration of intranasal NEs decreased in untargeted organs (heart, liver, spleen and kidney), and this result can not only improve the efficacy but also reduce the toxic side effects of the drug. HupA is a reversible and selective inhibitor of acetylcholinesterase (AChE) resulting in bradycardia, heart block and prolonged QT interval.[51] It is reported that there was once a case of acute renal failure related to HupA in China.[52]

The prepared intranasal nanoformulations of HupA-NE and Lf-HupA-NE in this paper showed different pharmacokinetic characteristics of drug absorption, distribution and elimination in vivo compared with those of conventional oral formulations. The Tmax, Cmax and AUC (0-t) of the nasal nanoformulations were significantly higher than those of the gavage administration in brain tissue. The intranasal NEs continuously accumulated HupA absorption to the brain. The increase in MRT(0-t) and $t_{1/2}$ in the brain and the decrease in CL/F prolonged the duration of action of the drug with sustained release. The small particle size of NEs plays a crucial role in pharmacokinetics, in which the residence times are prolonged.[53] In the heart, liver and kidney tissues, the nasal nanoformulations reduced the absorption and distribution of the drug. The nasal HupA-NE and Lf-HupA-NE increased the elimination rate of the drug and accelerated the elimination of the drug in the liver, kidney and spleen. Pharmacokinetic parameters showed that Lf-HupA-NE exhibited significant advantages in rapid absorption, high concentration, long retention time, large area under the curve and low clearance rate. The results of Ce (Ce HupA-NE=3.38, Ce Lf-HupA-NE=3.83) indicated that intranasal HupA-NE and Lf-HupA-NE resulted in an increased distribution and concentration of the drug in the brain compared to that of the HupA solution. Re HupA-NE=4.32 and Re Lf-HupA-NE=8.57 (Re>1) revealed that the drug formulations were targeted to the brain; in general, a higher Re value indicates more effective targeting of drugs. Ce and Re showed that HupA-NE and Lf-HupA-NE can be used as intracerebral drug delivery systems. The DTI=2.6 for Lf-HupA-NE demonstrated the superiority of Lf as a functional brain-targeting molecule. In the context of targeted therapy, ligands can bind to brain endothelial cells and neurons with high affinity and specificity. Lf-HupA-NE is more targeted to the brain and can improve the capacity of BBB transport.

## Conclusion

This study provided evidence indicating that some small integral NEs entered the brain by the nose-to-brain pathways, which comprise the nerve pathway (the main pathway) and the blood circulation route. An in vivo efflux study implied that P-gp, MRP1, and BCRP were involved in the development of resistance to HupA during the treatment of AD. Utilizing the HupA-NE system may be an effective strategy for enhancing drug absorption with a controlled efflux and increasing the concentration of drugs in the brain. Nasally administered HupA-NE and Lf-HupA-NE exhibited improved pharmacokinetic and brain-targeting parameters compared to those of the gavage HupA aqueous solution. Furthermore, the special organic distribution of NEs also reduced non-targeted organs toxicity of the HupA.

## Acknowledgments

The authors acknowledge Prof. Wei Wu and Dr Liwei Zhao at School of Pharmacy, Fudan University for providing probes.

## Funding

This work was supported by the WU JIEPING MEDICAL FOUNDATION. (No.320.6750.19089-41).

## Disclosure

The authors report no conflicts of interest in this work.

## References


1. Wen MM, El-Salamouni NS, El-Refaie WM, et al. Nanotechnology-based drug delivery systems for Alzheimer's disease management: technical, industrial, and clinical challenges. *J Control Release*. 2017;245:95–107. doi:10.1016/j.jconrel.2016.11.025
2. Klimova B, Kuca K. Alzheimer's disease and Chinese medicine as a useful alternative intervention tool: a mini-review. *Curr Alzheimer Res*. 2017;14(6):680–685. doi:10.2174/1567205014666170117103656
3. Agrawal M, Saraf S, Saraf S, et al. Nose-to-brain drug delivery: an update on clinical challenges and progress towards approval of anti-Alzheimer drugs. *J Control Release*. 2018;281:139–177. doi:10.1016/j.jconrel.2018.05.011
4. Ahmad N, Amin S, Neupane YR, Kohli K. Anal fissure nanocarrier of lercanidipine for enhanced transdermal delivery: formulation optimization, ex vivo and in vivo assessment. *Expert Opin Drug Deliv*. 2014;11(4):467–478. doi:10.1517/17425247.2014.876004
5. Dubois B, Feldman HH, Jacova C, et al. Revising the definition of Alzheimer's disease: a new lexicon. *Lancet Neurol*. 2010;9(11):1118–1127. doi:10.1016/S1474-4422(10)70223-4
6. Bhavna MS, Ali M, Ali M, et al. Donepezil nanosuspension intended for nose to brain targeting: in vitro and in vivo safety evaluation. *Int J Biol Macromol*. 2014;67:418–425. doi:10.1016/j.ijbiomac.2014.03.022
7. Tao T, Zhao Y, Yue P, Dong WX, Chen QH. 石杉碱甲鼻用原位凝胶的制备及其经鼻脑靶向性评价. *Yao Xue Xue Bao*. 2006;41(11):1104–1110. chinese. doi:10.16438/j.0513-4870.2006.11.015
8. Chen S, Zhang J, Wu L, Wu H, Dai M. Paeonol nanoemulsion for enhanced oral bioavailability: optimization and mechanism. *Nanomedicine*. 2018;13(3):269–282. doi:10.2217/nnm-2017-0277
9. Wanek T, Mairinger S, Langer O. Radioligands targeting P-glycoprotein and other drug efflux proteins at the blood-brain barrier. *J Labelled Comp Radiopharm*. 2013;56(3–4):68–77. doi:10.1002/jlcr.2993
10. Illum L. Nasal drug delivery–possibilities, problems and solutions. *J Control Release*. 2003;87(1–3):187–198. doi:10.1016/S0168-3659(02)00363-2
11. Chapman CD, Frey WH 2nd, Craft S, et al. Intranasal treatment of central nervous system dysfunction in humans. *Pharm Res*. 2013;30(10):2475–2484. doi:10.1007/s11095-012-0915-1
12. Chen XQ, Fawcett JR, Rahman YE, Ala TA, Frey IW. Delivery of nerve growth factor to the brain via the olfactory pathway. *J Alzheimers Dis*. 1998;1(1):35–44. doi:10.3233/JAD-1998-1102
13. Malerba F, Paoletti F, Capsoni S, Cattaneo A. Intranasal delivery of therapeutic proteins for neurological diseases. *Expert Opin Drug Deliv*. 2011;8(10):1277–1296. doi:10.1517/17425247.2011.588204
14. Turker S, Onur E, Ozer Y. Nasal route and drug delivery systems. *Pharm World Sci*. 2004;26(3):137–142. doi:10.1023/B:PHAR.0000026823.82950.ff
15. Chatterjee B, Gorain B, Mohananaidu K, Sengupta P, Mandal UK, Choudhury H. Targeted drug delivery to the brain via intranasal nanoemulsion: available proof of concept and existing challenges. *Int J Pharm*. 2019;565:258–268. doi:10.1016/j.ijpharm.2019.05.032
16. Pathak K, Akhtar N. Nose to brain delivery of nanoformulations for neurotherapeutics in Parkinson's disease: defining the preclinical, clinical and toxicity issues. *Curr Drug Deliv*. 2016;13(8):1205–1221. doi:10.2174/1567201813666160607123409
17. Li Y, Wang C, Zong S, et al. The trigeminal pathway dominates the nose-to-brain transportation of intact polymeric nanoparticles: evidence from aggregation-caused quenching probes. *J Biomed Nanotechnol*. 2019;15(4):686–702. doi:10.1166/jbn.2019.2724
18. He H, Xie Y, Lv Y, et al. Bioimaging of intact polycaprolactone nanoparticles using aggregation-caused quenching probes: size-dependent translocation via oral delivery. *Adv Healthc Mater*. 2018;7(22):e1800711. doi:10.1002/adhm.201800711
19. Ahmad E, Feng Y, Qi J, et al. Evidence of nose-to-brain delivery of nanoemulsions: cargoes but not vehicles. *Nanoscale*. 2017;9(3):1174–1183. doi:10.1039/C6NR07581A
20. Singh I, Swami R, Pooja D, Jeengar MK, Khan W, Sistla R. Lactoferrin bioconjugated solid lipid nanoparticles: a new drug delivery system for potential brain targeting. *J Drug Target*. 2016;24(3):212–223. doi:10.3109/1061186X.2015.1068320
21. Jiang Y, Liu C, Zhai W, Zhuang N, Han T, Ding Z. The optimization design of lactoferrin loaded HupA nanoemulsion for targeted drug transport via intranasal route. *Int J Nanomed*. 2019;14:9217–9234. doi:10.2147/IJN.S214657
22. Rautio J, Laine K, Gynther M, Savolainen J. Prodrug approaches for CNS delivery. *AAPS J*. 2008;10(1):92–102. doi:10.1208/s12248-008-9009-8
23. Zhao Y, Yue P, Tao T, Chen QH. Drug brain distribution following intranasal administration of Huperzine A in situ gel in rats. *Acta Pharmacol Sin*. 2007;28(2):273–278. doi:10.1111/j.1745-7254.2007.00486.x
24. Zhu XN, He P, Zhang L, et al. FBXO22 mediates polyubiquitination and inactivation of LKB1 to promote lung cancer cell growth. *Cell Death Dis*. 2019;10(7):486. doi:10.1038/s41419-019-1732-9
25. Tan SL, Stanslas J, Basri M, et al. Nanoemulsion-based parenteral drug delivery system of carbamazepine: preparation, characterization, stability evaluation and blood-brain pharmacokinetics. *Curr Drug Deliv*. 2015;12(6):795–804. doi:10.2174/1567201812666150901112544
26. Comfort C, Garrastazu G, Pozzoli M, Sonvico F. Opportunities and challenges for the nasal administration of nanoemulsions. *Curr Top Med Chem*. 2015;15(4):356–368. doi:10.2174/1568026615666150108144655
27. Meng Q, Wang A, Hua H, et al. Intranasal delivery of Huperzine A to the brain using lactoferrin-conjugated N-trimethylated chitosan surface-modified PLGA nanoparticles for treatment of Alzheimer's disease. *Int J Nanomed*. 2018;13:705–718. doi:10.2147/IJN.S151474
28. Suzuki YA, Lopez V, Lonnerdal B. Mammalian lactoferrin receptors: structure and function. *Cell Mol Life Sci*. 2005;62(22):2560–2575. doi:10.1007/s00018-005-5371-1
29. Elfinger M, Maucksch C, Rudolph C. Characterization of lactoferrin as a targeting ligand for nonviral gene delivery to airway epithelial cells. *Biomaterials*. 2007;28(23):3448–3455. doi:10.1016/j.biomaterials.2007.04.011
30. Qian ZM, Wang Q. Expression of iron transport proteins and excessive iron accumulation in the brain in neurodegenerative disorders. *Brain Res Brain Res Rev*. 1998;27(3):257–267. doi:10.1016/S0165-0173(98)00012-5
31. Liu Z, Jiang M, Kang T, et al. Lactoferrin-modified PEG-co-PCL nanoparticles for enhanced brain delivery of NAP peptide following intranasal administration. *Biomaterials*. 2013;34(15):3870–3881. doi:10.1016/j.biomaterials.2013.02.003
32. Guo C, Yang ZH, Zhang S, et al. Intranasal lactoferrin enhances alpha-secretase-dependent amyloid precursor protein processing via the ERK1/2-CREB and HIF-1alpha pathways in an alzheimer's disease mouse model. *Neuropsychopharmacology*. 2017;42(13):2504–2515. doi:10.1038/npp.2017.8
33. Bi C, Wang A, Chu Y, et al. Intranasal delivery of rotigotine to the brain with lactoferrin-modified PEG-PLGA nanoparticles for Parkinson's disease treatment. *Int J Nanomed*. 2016;11:6547–6559. doi:10.2147/IJN.S120939

34. Kakumanu S, Tagne JB, Wilson TA, Nicolosi RJ. A nanoemulsion formulation of dacarbazine reduces tumor size in a xenograft mouse epidermoid carcinoma model compared to dacarbazine suspension. *Nanomedicine*. 2011;7(3):277–283. doi:10.1016/j.nano.2010.12.002
35. Arora P, Sharma S, Garg S. Permeability issues in nasal drug delivery. *Drug Discov Today*. 2002;7(18):967–975. doi:10.1016/S1359-6446(02)02452-2
36. Alexander A, Saraf S. Nose-to-brain drug delivery approach: a key to easily accessing the brain for the treatment of Alzheimer's disease. *Neural Regen Res*. 2018;13(12):2102–2104. doi:10.4103/1673-5374.241458
37. Crowe TP, Greenlee MHW, Kanthasamy AG, Hsu WH. Mechanism of intranasal drug delivery directly to the brain. *Life Sci*. 2018;195:44–52. doi:10.1016/j.lfs.2017.12.025
38. Erdo F, Bors LA, Farkas D, Bajza A, Gizurarson S. Evaluation of intranasal delivery route of drug administration for brain targeting. *Brain Res Bull*. 2018;143:155–170. doi:10.1016/j.brainresbull.2018.10.009
39. Bonaccorso A, Musumeci T, Serapide MF, Pellitteri R, Uchegbu IF, Puglisi G. Nose to brain delivery in rats: effect of surface charge of rhodamine B labeled nanocarriers on brain subregion localization. *Colloids Surf B Biointerfaces*. 2017;154:297–306. doi:10.1016/j.colsurfb.2017.03.035
40. Graff CL, Pollack GM. P-Glycoprotein attenuates brain uptake of substrates after nasal instillation. *Pharm Res*. 2003;20(8):1225–1230. doi:10.1023/A:1025053115583
41. Hada N, Netzer WJ, Belhassan F, Wennogle LP, Gizurarson S. Nose-to-brain transport of imatinib mesylate: a pharmacokinetic evaluation. *Eur J Pharm Sci*. 2017;102:46–54. doi:10.1016/j.ejps.2017.02.032
42. Thorne RG, Pronk GJ, Padmanabhan V, Frey WH 2nd. Delivery of insulin-like growth factor-I to the rat brain and spinal cord along olfactory and trigeminal pathways following intranasal administration. *Neuroscience*. 2004;127(2):481–496. doi:10.1016/j.neuroscience.2004.05.029
43. Bors LA, Bajza A, Mandoki M, et al. Modulation of nose-to-brain delivery of a P-glycoprotein (MDR1) substrate model drug (quinidine) in rats. *Brain Res Bull*. 2020;160:65–73. doi:10.1016/j.brainresbull.2020.04.012
44. Pandey G, Mittapelly N, Valicherla GR, et al. P-gp modulatory acetyl-11-keto-beta-boswellic acid based nanoemulsified carrier system for augmented oral chemotherapy of docetaxel. *Colloids Surf B Biointerfaces*. 2017;155:276–286. doi:10.1016/j.colsurfb.2017.04.028
45. Ganta S, Singh A, Rawal Y, et al. Formulation development of a novel targeted theranostic nanoemulsion of docetaxel to overcome multidrug resistance in ovarian cancer. *Drug Deliv*. 2016;23(3):968–980. doi:10.3109/10717544.2014.923068
46. Werle M. Natural and synthetic polymers as inhibitors of drug efflux pumps. *Pharm Res*. 2008;25(3):500–511. doi:10.1007/s11095-007-9347-8
47. Al-Ali AA, Nielsen RB, Steffansen B, Holm R, Nielsen CU. Nonionic surfactants modulate the transport activity of ATP-binding cassette (ABC) transporters and solute carriers (SLC): relevance to oral drug absorption. *Int J Pharm*. 2019;566:410–433. doi:10.1016/j.ijpharm.2019.05.033
48. Hu P, Zhao F, Wang J, Zhu W. Lactoferrin attenuates lipopolysaccharide-stimulated inflammatory responses and barrier impairment through the modulation of NF-kappaB/MAPK/Nrf2 pathways in IPEC-J2 cells. *Food Funct*. 2020;11(10):8516–8526. doi:10.1039/D0FO01570A
49. Wu J, Zhu Y, Li F, et al. Spica prunellae and its marker compound rosmarinic acid induced the expression of efflux transporters through activation of Nrf2-mediated signaling pathway in HepG2 cells. *J Ethnopharmacol*. 2016;193:1–11. doi:10.1016/j.jep.2016.07.021
50. Lou Y, Guo Z, Zhu Y, et al. Astragali radix and its main bioactive compounds activate the Nrf2-mediated signaling pathway to induce P-glycoprotein and breast cancer resistance protein. *J Ethnopharmacol*. 2019;228:82–91. doi:10.1016/j.jep.2018.09.026
51. Zhang J, He Y, Jiang X, Jiang H, Shen J. Nature brings new avenues to the therapy of central nervous system diseases-An overview of possible treatments derived from natural products. *Sci China Life Sci*. 2019;62(10):1332–1367. doi:10.1007/s11427-019-9587-y
52. Zhao Y, Huang F, Chen J. 口服石杉碱甲致急性肾功能衰竭死亡1例. *Chin J New Drugs*. 2006;15(15):1305–1306.
53. Fan W, Yu Z, Peng H, et al. Effect of particle size on the pharmacokinetics and biodistribution of parenteral nanoemulsions. *Int J Pharm*. 2020;586:119551. doi:10.1016/j.ijpharm.2020.119551